

Electronic Supporting Information (ESI) for

Enhancing Phosphorescence of Hybrid Metal Halides through Molecular Sensitization

Liao-Kuo Gong,^{a, c} Jian-Rong Li,^a Zhao-Feng Wu,^a Bing Hu,^a Ze-Ping Wang,^a Nan-Nan Shen,^a Qian-Qian Hu,^a Zhong-Hua Deng,^a Zhi-Zhuan Zhang,^{a, b} Jing-Jing Fu,^a Ke-Zhao Du^{,b} and Xiao-Ying Huang^{*,a}*

^a *State Key Laboratory of Structure Chemistry, Fujian Institute of Research on the Structure of Matter, Chinese Academy of Sciences, Fuzhou 350002, China.*

^b *College of Chemistry and Materials Science, Fujian Provincial Key Laboratory of Advanced Materials Oriented Chemical Engineering, Fujian Normal University, 32 Shangsang Road, Fuzhou 350007, China.*

^c *University of Chinese Academy of Sciences, Beijing, 100049, China.*

E-mail: xyhuang@fjirsm.ac.cn; duke@fjnu.edu.cn

Table of Contents

Table S1 Crystallographic data for [BPy]₆[Pb₃Br₁₂] (BPB).

Table S2 The average values of lifetimes and QYs for different thiadiazole-sensitized BPBs.

Table S3 Phosphorescence lifetimes (τ_p) obtained from fitting the decay curves.

Table S4 The Commission International de l'Eclairage color coordinates (CIEs) and correlated color temperatures (CCTs) of $x\%$ MTT@BPBs.

Table S5 The S contents in $x\%$ MTT@BPBs determined by ICP.

Table S6 The Stoke shift values of $x\%$ MTT@BPBs.

Fig. S1 Crystal structural diagrams for [BPy]₆[Pb₃Br₁₂] (BPB, BPy = N-butyl pyridinium cation); yellow dashed lines represent the H-bonds.

Fig. S2 PXRD patterns of the $x\%$ MTT@BPBs.

Fig. S3 TG curve of BPB.

Fig. S4 The time-resolved photoluminescence (TRPL) of [BPy]Br at 77K (a) and 298K (b).

Fig. S5 Crystal photographs of BPB and 2.21%MTT@BPB.

Fig. S6 The total X-ray photoelectron spectroscopy of BPB and 5.81%MTT@BPB (a), Pb 4f (b) and S 2p (c).

Fig. S7 Photos of BPB crystals sensitized by different MTT concentrations without and with 365nm excitation, respectively.

Fig. S8 The Commission International de l'Eclairage color coordinates (CIEs) and correlated color temperatures (CCTs) of the $x\%$ MTT@BPBs.

Fig. S9 PL spectra of 5.81% MTT@BPB crystals and the corresponding thin film.

Fig. S10 (a) Solid-state PL spectra of the as-fabricated WLED; inset: The CIE chromaticity diagram; the photographs of the as-fabricated WLED before (b) and after (c) illumination.

Experimental Procedures

Materials

Lead bromide (PbBr₂, 99.0%, Macklin), N-butyl pyridinium bromide ([BPy]Br, 99%, Lanzhou Greenchem ILs), 5-Methyl-1,3,4-thiadiazole-2-thiol (MTT, > 98.0%, Tokyo Chemical Industry Co., Ltd), N,N-Dimethylacetamide (DMA, ≥ 99.0%, Sinopharm), 2,5-Dimercapto-1,3,4-thiadiazole (DMT, > 98.0%, Alfa), 2-Amino-5-Methyl-1,3,4-Thiadiazole (AMT, 98%, Adamas), 2-Aminothiazole (2-AT, 98%, Adamas). All chemicals were used as received without further purification.

Synthesis

Growth of BPB Crystals. BPB was synthesized by the one-step solvothermal method. [BPy]Br (2 mmol), PbBr₂ (1 mmol), and DMA (4 mL) were added into a poly(tetrafluoroethylene) (Teflon) liner (28 mL) with stirring at room temperature. After 20 minutes stirring, the Teflon liner was transferred into a stainless steel autoclave and put in an oven. The autoclave was heated up to 120°C, maintained for 3 days, and cooled to room temperature naturally. Finally, the light brown block-like crystals were separated from the brown solution by filtration. The yield was about 46.87% (0.3746 g) based on the amount of PbBr₂. Anal. Calc. for Pb₃Br₁₂C₅₄H₈₄N₆: C, 27.05%; N, 3.50%; H, 3.53%; Found: C, 27.29%; N, 3.54%; H, 3.41%.

Growth of x% MTT@BPB Crystals. x% MTT@BPB crystals were synthesized using the same way with the additional certain amount of 5-Methyl-1,3,4-thiadiazole-2-thiol (MTT) (0.25 mmol, 0.50 mmol, 0.75 mmol, 1.00 mmol, 1.50 mmol, 2.00 mmol) in the starting materials to obtain the 0.37% MTT@BPB, 2.21% MTT@BPB, 2.41% MTT@BPB, 2.47% MTT@BPB, 5.81% MTT@BPB and 4.35% MTT@BPB, respectively.

Characterization methods

Single Crystal X-ray diffraction (SCXRD). A suitable BPB single crystal was carefully selected under an optical microscope and glued to a thin glass fiber. The single-crystal X-ray diffraction data was collected on a SuperNova CCD diffractometer with graphite-monochromated MoK α radiation ($\lambda = 0.71073 \text{ \AA}$) at 100(2) K. The structure was solved by direct methods and refined by full-matrix least-squares on F^2 using the SHELXL-2016 program package.^[1] All non-hydrogen atoms were refined anisotropically. Hydrogen atoms attached to C atoms were located at geometrically calculated positions and were not refined. The empirical formula was confirmed by element analysis (EA) results. CCDC no.1885136 contains the supplementary crystallographic data for this structure.

Powder X-ray diffraction (PXRD). The PXRD was measured on a Rigaku Miniflex-II diffractometer with CuK α radiation ($\lambda = 1.54178 \text{ \AA}$) in the angular range of $2\theta = 3\text{--}65^\circ$ with a scan speed of $2^\circ/\text{min}$. The PXRD simulated pattern is based on single-crystal X-ray diffraction data using the Mercury Powder Pattern Calculate program.^[2]

Elemental analysis (EA). EA was performed using a German Elementary Vario EL III instrument.

Solid state optical absorption spectra. Solid state diffuse reflectance spectra were recorded at room temperature using Shimadzu 2600 UV/Vis spectrometer in the range of 800~200 nm with a BaSO₄ plate as a reference (100% reflectance). The absorption data was calculated from the diffuse reflectance using the Kubelka-Munk function $\alpha/s = (1-R)^2/2R$. Where α is the absorption coefficient; S is the scattering coefficient and R is the diffuse reflectance.

Thermogravimetric analysis (TGA). TGA was performed on a NETZSCH STA 449F3 unit at a heating rate of $10 \text{ K}\cdot\text{min}^{-1}$ under N₂ atmosphere.

Electron spin resonance (ESR) spectra. ESR were recorded on a Bruker ER-420 spectrometer with a 100 kHz magnetic field in the X band at RT.

Inductively coupled plasma-optical emission spectroscopy (ICP-OES). ICP-OES was performed on a Thermo 7400. The concentration of S²⁻ was measured by dissolution of 0.10 g sample in 50 mL 2% wt HNO₃ aqueous solution by ICP-OES.

Photophysical properties. PL (photoluminescence), PLE (photoluminescence excitation) and TRPL (time-resolved photoluminescence) were recorded on Edinburgh FL980 UV/V/NIR fluorescence spectrometer. Quantum yield was measured by Edinburgh FLS 1000 UV/V/NIR fluorescence spectrometer.

Fabrication of WLED device. The BPB thin film on various substrates can be achieved using a melting-recrystallization method. The powder of 5.81% MTT@BPB was placed between two glass sheets, and then the glass sheets were placed on a heating plate at 170 °C for 20 min to obtain the melting compound. The temperature of the heating plate was then reduced to the room temperature with the speed of 1°C/min. Finally, the yellow phosphor film was obtained by melting-recrystallization. The white-light lamp was fabricated in the similar way. The molten 5.81% MTT@BPB was obtained on the heating plate at 170 °C. A blue lamp ($\lambda = 390\text{-}400$ nm) was inserted into the molten gel to coat the yellow phosphor materials (i.e. 5.81% MTT@BPB). After the recrystallization of the coating layer through naturally cooling, a white-light lamp was fabricated successfully. A finely powdered sample of 5.81% MTT@BPB was loaded onto a 0.2×0.6 mm LED chip ($\lambda = 380$ nm) by the melting-recrystallization method to produce the WLED. The parameters for the WLED were evaluated using a LED 300E system with a half-moon integrating sphere (MODEL 0.5 LED R98).

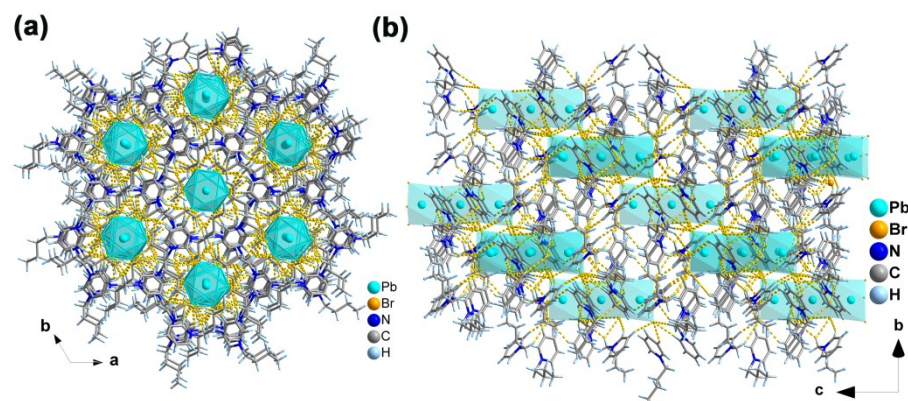


Fig. S1 Crystal structural diagrams of $[\text{BPy}]_6[\text{Pb}_3\text{Br}_{12}]$ (BPB, BPy = N-butyl pyridinium cation); yellow dashed lines represent the H-bonds.

Table S1 Crystallographic data for $[\text{BPy}]_6[\text{Pb}_3\text{Br}_{12}]$ (BPB).

Crystal	$[\text{BPy}]_6[\text{Pb}_3\text{Br}_{12}]$
Empirical formula	$\text{C}_{54}\text{H}_{84}\text{Br}_{12}\text{N}_6\text{Pb}_3$
Formula weight	2397.76
Crystal system	Trigonal
Space group	$R\bar{3}$
$a/\text{\AA}$	17.1167(6)
$b/\text{\AA}$	17.1167(6)
$c/\text{\AA}$	21.9553(12)
$V/\text{\AA}^3$	5570.7(5)
Z	3
T/K	100(2)
$F(000)$	3348
$\rho_{\text{calcd}}/\text{g cm}^{-3}$	2.144
μ/mm^{-1}	13.274
Measured refls.	6049
Independent refls.	2672
No. of parameters	115
R_{int}	0.0194
$R_1 (I > 2\sigma(I))^a$	0.0184
$wR (I > 2\sigma(I))^b$	0.0405
GOF	1.001
CCDC	1885136

[a] $R_1 = \frac{\sum \|F_o\| - \|F_c\|}{\sum \|F_o\|}$, [b] $wR_2 = \left[\frac{\sum w(F_o^2 - F_c^2)^2}{\sum w(F_o^2)^2} \right]^{1/2}$.

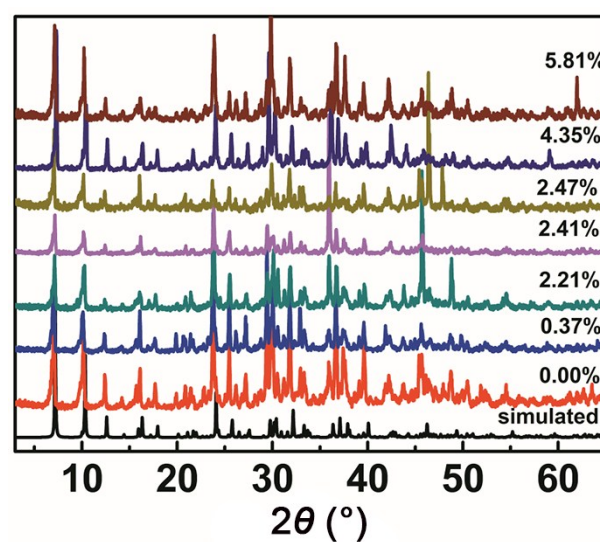


Fig. S2 PXRD patterns of the $x\%$ MTT@BPBs.

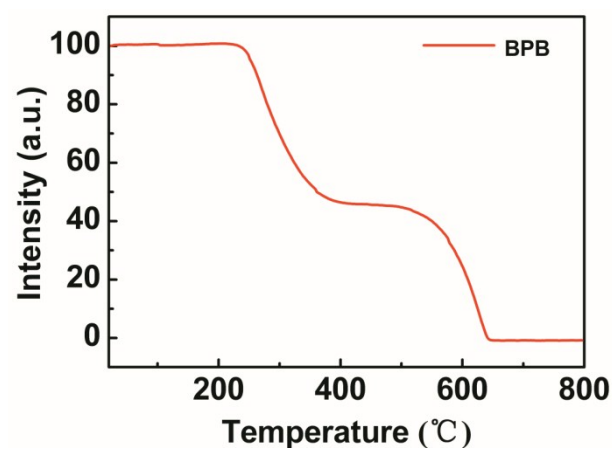


Fig. S3 TG curve of BPB. The melting point of BPB was recorded by hand (through observing the crystal state change at different temperatures starting from the room temperature).

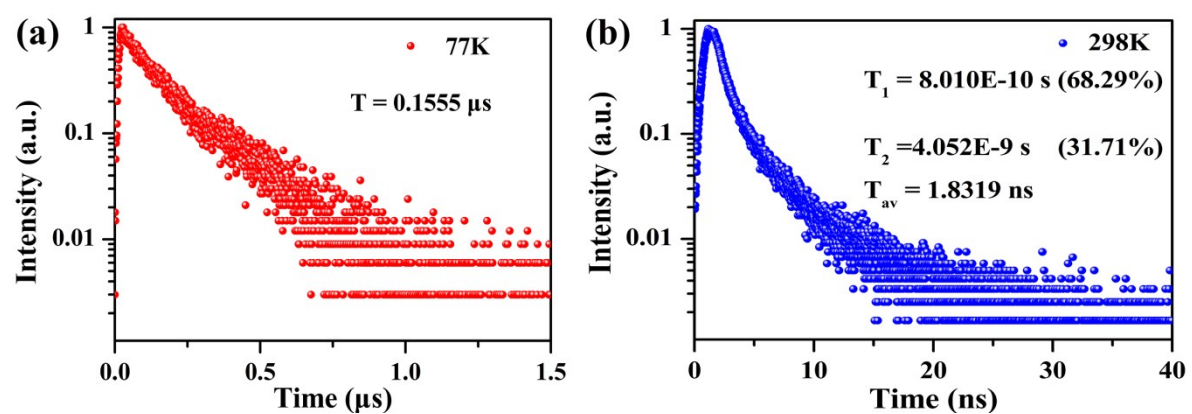


Fig. S4 The time-resolved photoluminescence (TRPL) of [BPY]Br at 77K (a) and 298K (b).



Fig. S5 Crystal photographs of BPB and 2.21%MTT@BPB.

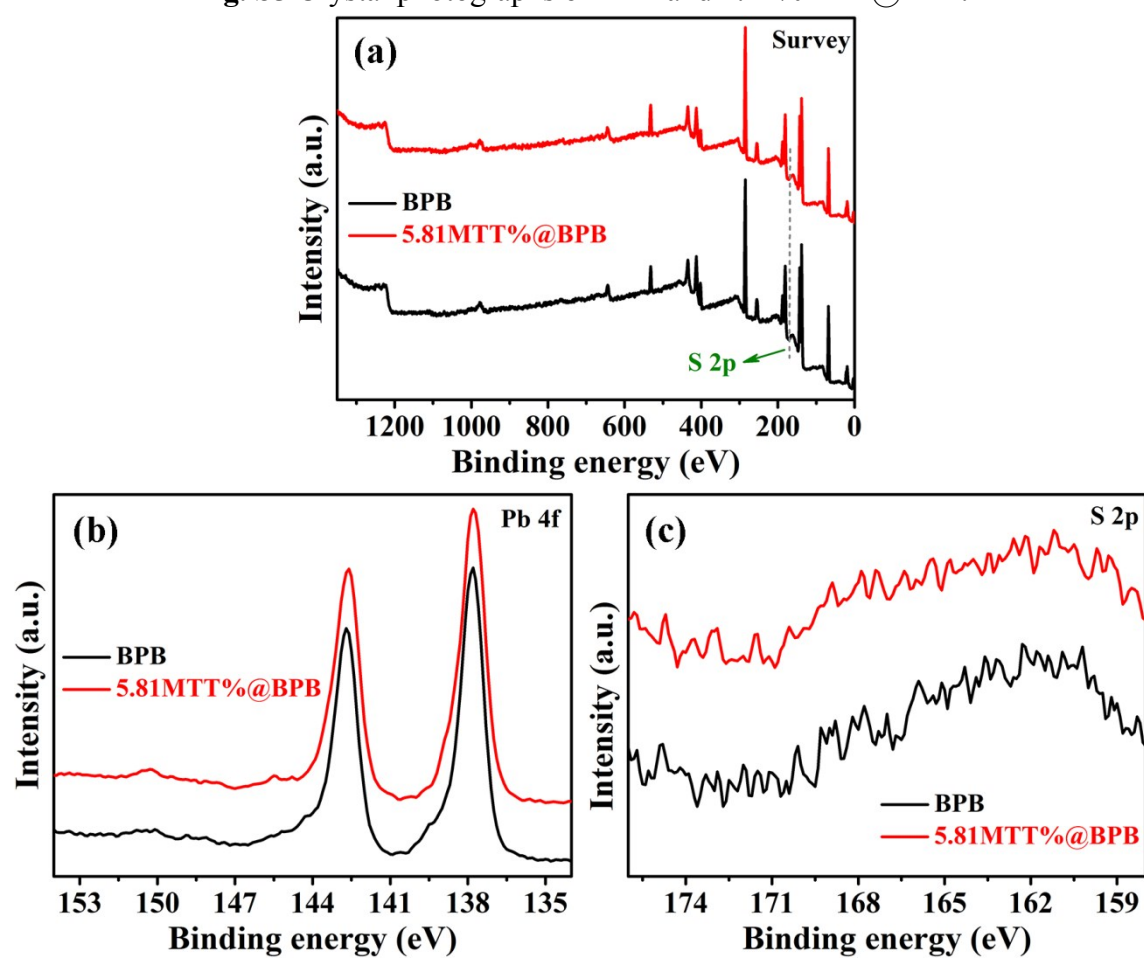


Fig. S6 The total X-ray photoelectron spectroscopy (a), Pb 4f (b) and S 2p (c) of BPB and 5.81%MTT@BPB.

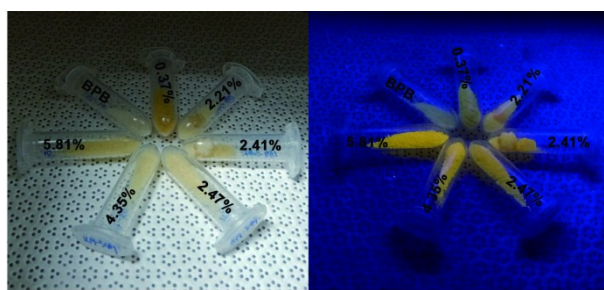
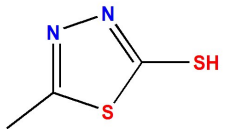


Fig. S7 Photos of BPB crystals sensitized by MTT with different concentrations without and with 365 nm excitation, respectively.

Table S2 The average values of lifetimes and QYs of different thiadiazole-sensitized BPBs.

L	τ_{av} (s)	QY(%)
 5-Methyl-1,3,4-thiadiazole-2-thiol	1.615E-3	2.81%

	1.357E-7	2.08%
	1.020E-7	2.14%
	1.354E-7	1.65%

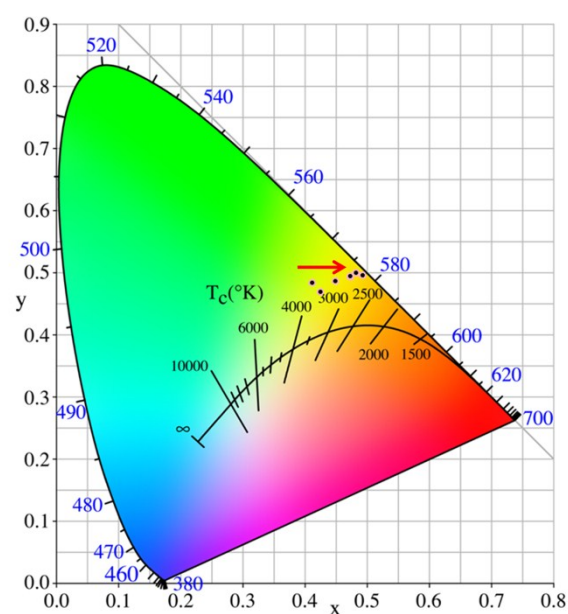


Fig. S8 The Commission International de l'Eclairage color coordinates (CIEs) and correlated color temperatures (CCTs) of the $x\%$ MTT@BPB.

Table S3 Phosphorescence lifetimes (τ) obtained from fitting the decay curves.

	τ_1 (s)	A_1	τ_2 (s)	A_2	τ_{av} (s)	QY(1,%)	QY(2,%)
TTA	8.112E-10	0.6837	6.586E-9	0.3163	2.638E-9	<1%	<1%
[BPy]Br	8.010E-10	0.6829	4.052E-9	0.3171	1.832E-9	<1%	<1%
PbBr ₂	3.897E-10	0.7835	4.062E-9	0.2165	1.185E-9	<1%	<1%
0%	9.503E-4	0.3677	6.124E-3	0.6323	4.222E-3	0.94	0.78
0.37%	2.501E-4	0.4754	2.995E-3	0.5246	1.690E-3	2.76	2.11
2.21%	2.240E-4	0.3885	3.516E-3	0.6115	2.237E-3	2.81	2.50
2.41%	2.310E-4	0.2570	4.387E-3	0.7430	3.320E-3	3.36	3.44
2.47%	1.689E-4	0.3777	4.178E-3	0.6223	2.664E-3	2.30	4.40
4.35%	1.480E-4	0.3963	4.928E-3	0.6037	3.034E-3	7.71	7.78
5.81%	1.651E-4	0.3805	4.141E-3	0.6195	2.628E-3	13.70	10.61

Note: For the accuracy of the data, the quantum yield was tested twice.

Table S4 The Commission International de l'Eclairage color coordinates (CIEs) and correlated color temperatures (CCTs) of $x\%$ MTT@BPB.

	CIE	CCT (T/K)
BPB	(0.426, 0.469)	3603K
0.37% MTT@BPB	(0.412, 0.484)	3932K
2.21% MTT@BPB	(0.450, 0.487)	3323K
2.41% MTT@BPB	(0.473, 0.494)	3038K
2.47% MTT@BPB	(0.474, 0.495)	3031K
4.35% MTT@BPB	(0.483, 0.500)	2945
5.81% MTT@BPB	(0.493, 0.496)	2795K

Table S5 The S contents in $x\%$ MTT@BPBs determined by ICP.

Doping concentration	ICP (S, mg/L)	n(MTT)/n(BPB)(%)
----------------------	---------------	------------------

	n(MTT)/n(BPB)(%)		
0 mmol	0	0	0
0.25 mmol	75.33	0.087	0.37014
0.50 mmol	149.76	1.069	2.20589
0.75 mmol	224.87	1.209	2.4676
1.00 mmol	300.66	1.179	2.41152
1.50 mmol	450.65	2.999	5.81382
2.00 mmol	599.50	2.219	4.35569

Table S6 The stoke shift values of x% MTT@BPBs.

	λ_{ex} (nm)	λ_{em} (nm)	ΔE_{ST} (ev)
BPB	342	583	1.501 (241 nm)
0.37% MTT@BPB	342	575	1.472 (233 nm)
2.21% MTT@BPB	362	575	1.271 (213 nm)
2.41% MTT@BPB	388	575	1.041 (187 nm)
2.47% MTT@BPB	390	573	1.017 (183 nm)
4.35% MTT@BPB	391	572	1.005 (181 nm)
5.81% MTT@BPB	391	570	0.998 (179 nm)

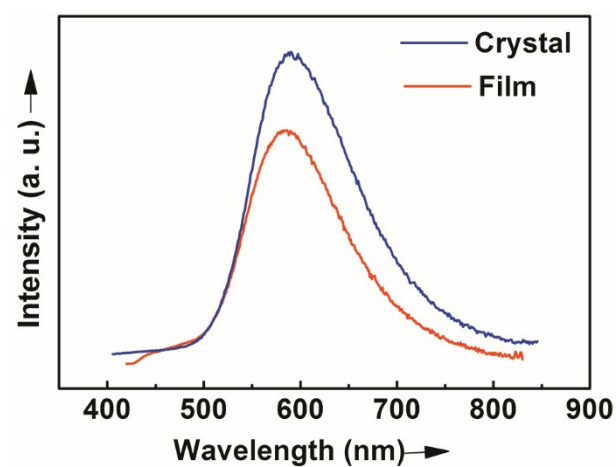


Fig. S9 PL spectra of 5.81% MTT@BPB crystals and the corresponding thin film.

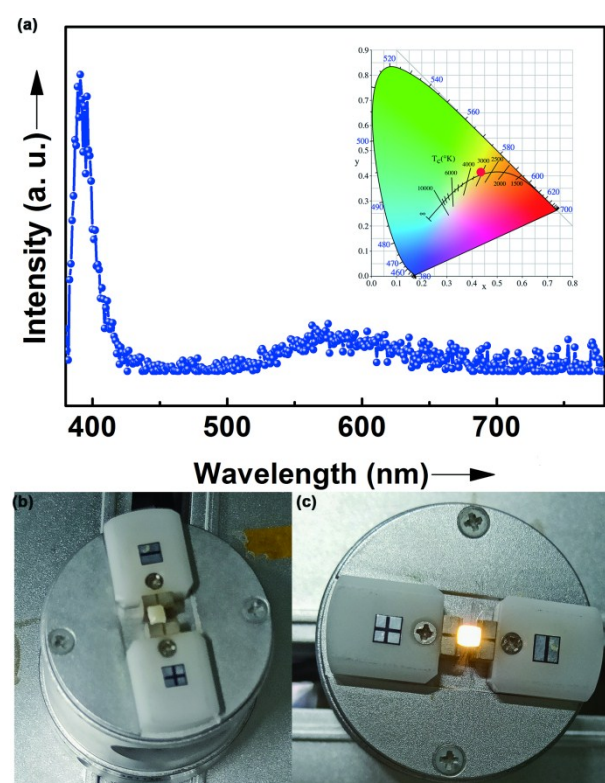


Fig. S10 (a) Solid-state PL spectra of the as-fabricated WLED; inset: The CIE chromaticity diagram; photographs of the as-fabricated WLED before (b) and after (c) illumination.

References

- [1] G. M. Sheldrick, *Acta Crystallogr. Sect. C-Struct. Chem.* **2015**, 71, 3-8.
- [2] <http://www.ccdc.cam.ac.uk/mercury/>